

The Fermi surface and band folding in  $\text{La}_{2-x}\text{Sr}_x\text{CuO}_4$ , probed by angle-resolved photoemission

This article has been downloaded from IOPscience. Please scroll down to see the full text article.

2010 New J. Phys. 12 125003

(<http://iopscience.iop.org/1367-2630/12/12/125003>)

View [the table of contents for this issue](#), or go to the [journal homepage](#) for more

Download details:

IP Address: 132.68.75.97

The article was downloaded on 05/11/2012 at 12:59

Please note that [terms and conditions apply](#).

## The Fermi surface and band folding in $\text{La}_{2-x}\text{Sr}_x\text{CuO}_4$ , probed by angle-resolved photoemission

E Razzoli<sup>1,2</sup>, Y Sassa<sup>3</sup>, G Drachuck<sup>4</sup>, M Månsson<sup>2,3</sup>, A Keren<sup>4</sup>, M Shay<sup>4</sup>, M H Berntsen<sup>5</sup>, O Tjernberg<sup>5</sup>, M Radovic<sup>1,2</sup>, J Chang<sup>3</sup>, S Pailhès<sup>6</sup>, N Momono<sup>7</sup>, M Oda<sup>8</sup>, M Ido<sup>8</sup>, O J Lipscombe<sup>9</sup>, S M Hayden<sup>9</sup>, L Patthey<sup>1</sup>, J Mesot<sup>2,3</sup> and M Shi<sup>1,10</sup>

<sup>1</sup> Swiss Light Source, Paul Scherrer Institut, CH-5232 Villigen PSI, Switzerland

<sup>2</sup> Laboratory for Synchrotron and Neutron Spectroscopy, EPF Lausanne, CH-1015 Lausanne, Switzerland

<sup>3</sup> Laboratory for Neutron Scattering, Paul Scherrer Institut, CH-5232 Villigen PSI, Switzerland

<sup>4</sup> Department of Physics, Technion-Israel Institute of Technology, Haifa 32000, Israel

<sup>5</sup> Materials Physics, KTH Royal Institute of Technology, S-16440 Kista, Sweden

<sup>6</sup> CEA, CNRS, CE Saclay, Laboratoire Léon Brillouin, F-91191 Gif Sur Yvette, France

<sup>7</sup> Department of Applied Sciences, Muroran Institute of Technology, Muroran 050-8585, Japan

<sup>8</sup> Department of Physics, Hokkaido University, Sapporo 060-0810, Japan

<sup>9</sup> H H Wills Physics Laboratory, University of Bristol, Tyndall Avenue, Bristol BS8 1TL, UK

E-mail: [ming.shi@psi.ch](mailto:ming.shi@psi.ch)

*New Journal of Physics* **12** (2010) 125003 (11pp)

Received 3 September 2010

Published 6 December 2010

Online at <http://www.njp.org/>

doi:10.1088/1367-2630/12/12/125003

**Abstract.** A systematic angle-resolved photoemission study of the electronic structure of  $\text{La}_{2-x}\text{Sr}_x\text{CuO}_4$  in a wide doping range is presented in this paper. In addition to the main energy band, we observed a weaker additional band, the  $(\pi, \pi)$  folded band, which shows unusual doping dependence. The appearance of the folded band suggests that a Fermi surface reconstruction is doping dependent and could already occur at zero magnetic field.

<sup>10</sup> Author to whom any correspondence should be addressed.

**Contents**

<b>1. Introduction</b>	<b>2</b>
<b>2. Angle-resolved photoemission spectroscopy (ARPES) measurements</b>	<b>2</b>
<b>3. ARPES results</b>	<b>3</b>
3.1. Fermi surface (FS) of $\text{La}_{2-x}\text{Sr}_x\text{CuO}_4$ . . . . .	3
3.2. The $(\pi, \pi)$ folded band and its FS of the highly underdoped samples . . . . .	5
<b>4. Discussion</b>	<b>7</b>
<b>5. Summary</b>	<b>9</b>
<b>Acknowledgments</b>	<b>10</b>
<b>References</b>	<b>10</b>

**1. Introduction**

Since the discovery of high-temperature cuprate superconductors, the study of the Fermi surface (FS) and its low-energy quasi-particle excitations has attracted much attention [1, 2]. This is because information on low-energy excitations near the FS is essential for understanding the unusual doping dependence of physical properties in cuprates and how high-temperature superconductivity emerges from a doped Mott insulator. The FS is a fundamental property in the normal ‘metallic’ state of solids. It is composed of the set of points in momentum ( $k$ -) space describing gapless electronic excitations and differentiating filled from unfilled states. The FS can be measured by angle-resolved photoemission spectroscopy (ARPES), which probes electronic excitations as a function of momentum and energy. The shape and size of the FS can also be inferred from quantum oscillation measurements. While both techniques have confirmed the existence of a large FS in overdoped cuprates [3, 4], they give topologically different FSs in underdoped materials. Quantum oscillation experiments reveal the existence of an FS comprising small (multiple) pockets [5, 6]. By contrast, photoemission experiments on underdoped cuprates instead reveal either disconnected gapless ‘Fermi arcs’ in the near nodal region [7, 8] or the coexistence of Fermi arcs and hole-like Fermi pockets [9], but the electron-like pocket suggested by a combination of quantum oscillation and Hall coefficient experiments [10] was not observed. An intriguing question is how to reconcile the different observations in these two types of measurements. FS reconstruction caused by the magnetic-field-induced superstructure [11, 12] as well as spin and charge modulation in the striped state [13] has been postulated to account for the small FS pockets inferred from quantum oscillations. In this paper, we present a comprehensive ARPES study of the electronic structure of  $\text{La}_{2-x}\text{Sr}_x\text{CuO}_4$  (LSCO) in a wide doping range, from non-superconducting insulating samples to highly doped superconducting ones. We show that while the main FS changes monotonically with adding more charge carriers to the system, a folded band that resembles a copy of the main band but shifted by  $(\pi, \pi)$  has unusual doping dependence. The appearance of the folded band suggests that an FS reconstruction could already occur at zero magnetic field and at low temperatures.

**2. Angle-resolved photoemission spectroscopy (ARPES) measurements**

ARPES experiments were carried out at the Surface and Interface Spectroscopy beamline at the Swiss Light Source on single crystals of LSCO with  $x = 0.03, 0.08, 0.12, 0.14, 0.17$

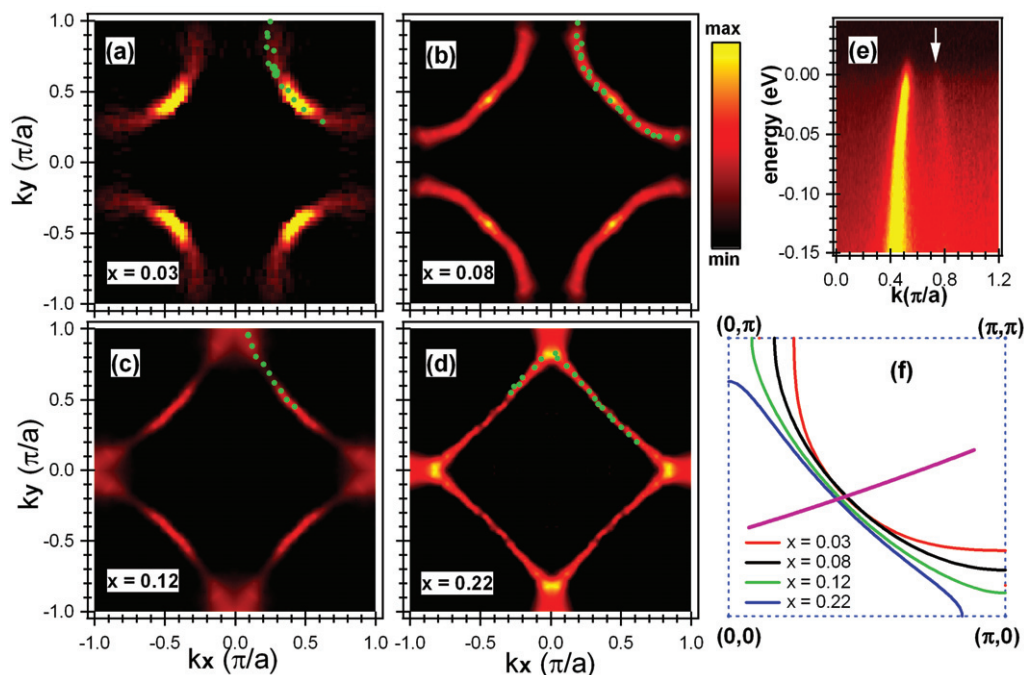


**Figure 1.** (a–d) Spectral weight map in  $k$ -space at  $E_F$  in LSCO. The data were obtained at  $T = 20$  K for the  $x = 0.03$  sample and at  $T = 12$  K for the rest of the samples. The doping levels ( $x$ ) are indicated at the lower left corner of each of (a–d). Circles are  $k_f$  determined from peak positions of the MDC at zero binding energy. (e) ARPES intensity plot, acquired from the  $x = 0.08$  sample, along the momentum cut indicated in (f) by the pink line. A second weaker band that disperses opposite to the main band (the left band) is indicated by an arrow. (f) The FS of the main band from tight-binding fits for different doping values.

and 0.22. The crystals were grown in traveling solvent floating zone furnaces. All samples were characterized by x-ray diffraction, and their superconducting transitions were determined by magnetization measurements. Circularly polarized light with a photon energy  $h\nu = 55$  eV was used in order to maximize the signal. The spectra were recorded with Scienta SES-2002 and R4000 analyzers. The energy and angle resolutions were  $\sim 17$  meV and  $0.1$ – $0.15^\circ$ , respectively. The Fermi level was determined by obtaining photoemission spectra from polycrystalline copper on the sample holder. The samples were cleaved *in situ* by using a specially designed cleaver [14]. Low-energy electron diffraction (LEED) analysis of the cleaved samples shows a clear  $(1 \times 1)$  pattern with no sign of surface reconstruction. During the measurements, the base pressure was less than  $5 \times 10^{-11}$  mbar at  $T < 40$  K and  $2 \times 10^{-10}$  mbar at  $T \sim 150$  K, respectively.

### 3. ARPES results

#### 3.1. Fermi surface (FS) of $La_{2-x}Sr_xCuO_4$

Figure 1 shows the spectral weight mapping in  $k$ -space at the Fermi level ( $E_F$ ) for selected doping values. The ARPES data were acquired in the first and the second Brillouin zone (BZ) at  $T = 12$  K for superconducting samples ( $x = 0.8, 0.12$  and  $0.22$ ,  $T_c = 20, 27$  and  $22$  K,

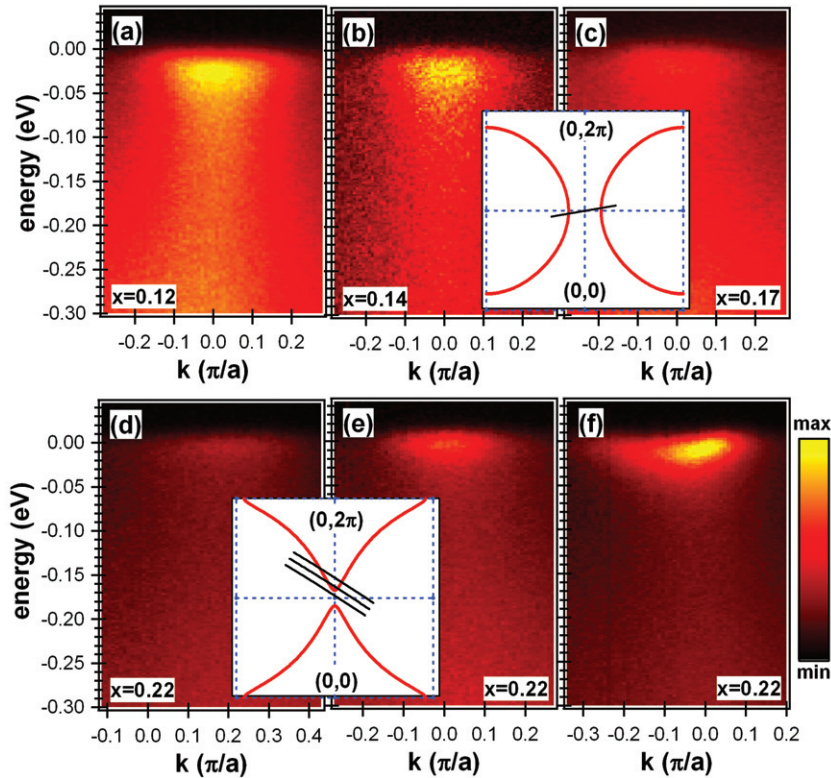


**Figure 2.** ARPES spectra of LSCO at  $T = 12$  K. (a–c) Intensity plots for  $x = 0.12$ ,  $0.14$  and  $0.17$  along the momentum cut indicated in the inset. (d–f) Intensity plots for  $x = 0.22$  along the three cuts, from bottom to top, shown in the inset.

respectively) and at  $T = 20$  K for the non-superconducting sample ( $x = 0.03$ ). The intensity maps (figures 1(a)–(d)) were constructed by reflection into the first BZ, using interpolation to a uniform grid and integrating the spectral weight in an energy window of 10 meV width centered at the  $E_F$ . The bright areas correspond to high intensity and represent the underlying FS—the minimum gap locus of the main band (the left band in figure 1(e)). The peak positions of the momentum distribution curves (MDCs) at zero binding energy are indicated by closed circles. These FSs are consistent with the observation in early studies [15]. The overdoped sample ( $x = 0.22$ ) displays an electron-like [16] FS. Upon underdoping FS topology changes from an electron-like pocket centered at the  $\Gamma$  point to a hole-like pocket centered at the  $(\pi, \pi)$  point, and by counting the number of holes per Cu atom the volume of FS decreases (figure 1(f)). A careful inspection of the spectra reveals that the topology of the FSs changes at a doping between  $x = 0.17$  and  $x = 0.22$ . In figure 2, we plot ARPES spectra in the vicinity of  $(0, \pi)$ . For dopings up to  $x = 0.17$ , the bottom of the energy band, located at  $(0, \pi)$ , lies below the  $E_F$ , which means that the FS is hole-like. This is in contrast to the observation for the  $x = 0.22$  sample, for which the bottom of the band becomes occupied only when the momentum cuts move away from the  $(0, \pi)$  point. This is clear evidence that the FS closes before reaching the zone boundary, i.e. electron-like.

We have investigated whether  $k_f$  changes with temperature for the most underdoped superconducting sample ( $x = 0.08$ ). Figures 3(c) and (d) show the MDCs at zero binding

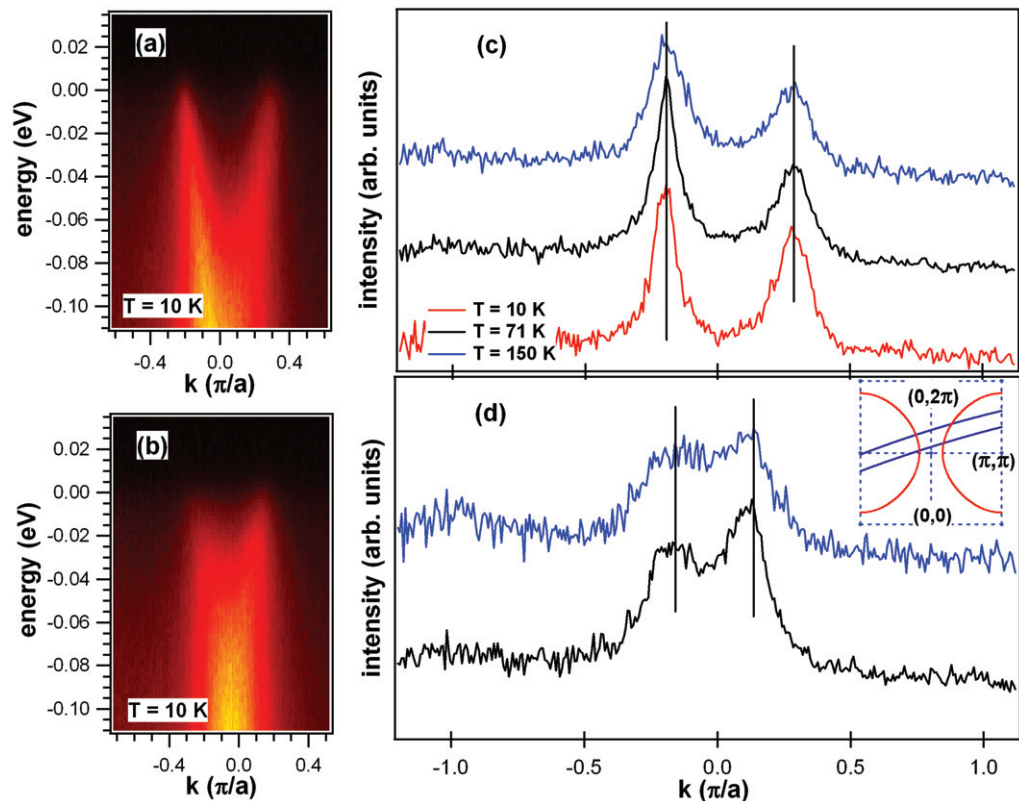


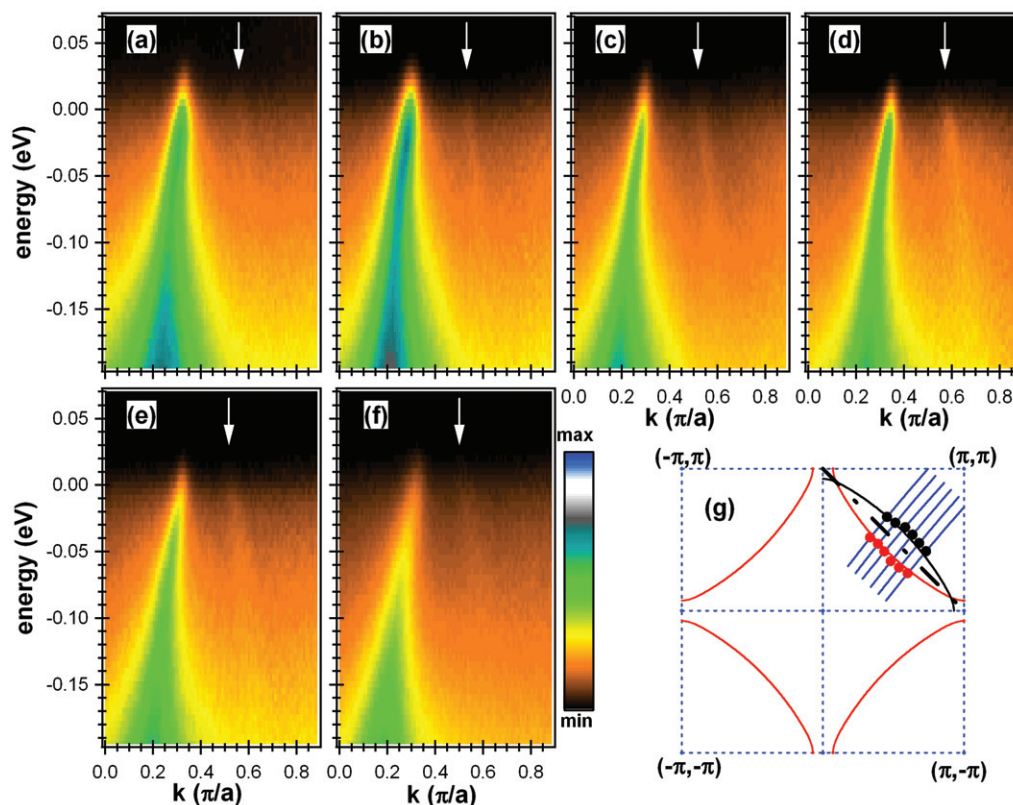
**Figure 3.** ARPES spectra of LSCO ( $x = 0.08$ ), acquired at several temperatures. (a and b) Intensity plots along the cuts (from top to bottom) indicated in the inset of (d). (c) MDCs at zero binding energy along the top cut in the inset of (d). (d) MDCs at zero binding energy along the bottom cut in the inset.

energy along two cuts that intersect with the underlying FS from near the node to near the anti-node. The well-defined MDC peak positions, from which the  $k_f$  were determined, remain unchanged at different temperatures, as is indicated by the vertical lines. This implies that the underlying FS in the superconducting state is the same as that at temperatures much higher than the superconducting transition temperature  $T_c$ .

### 3.2. The $(\pi, \pi)$ folded band and its FS of the highly underdoped samples

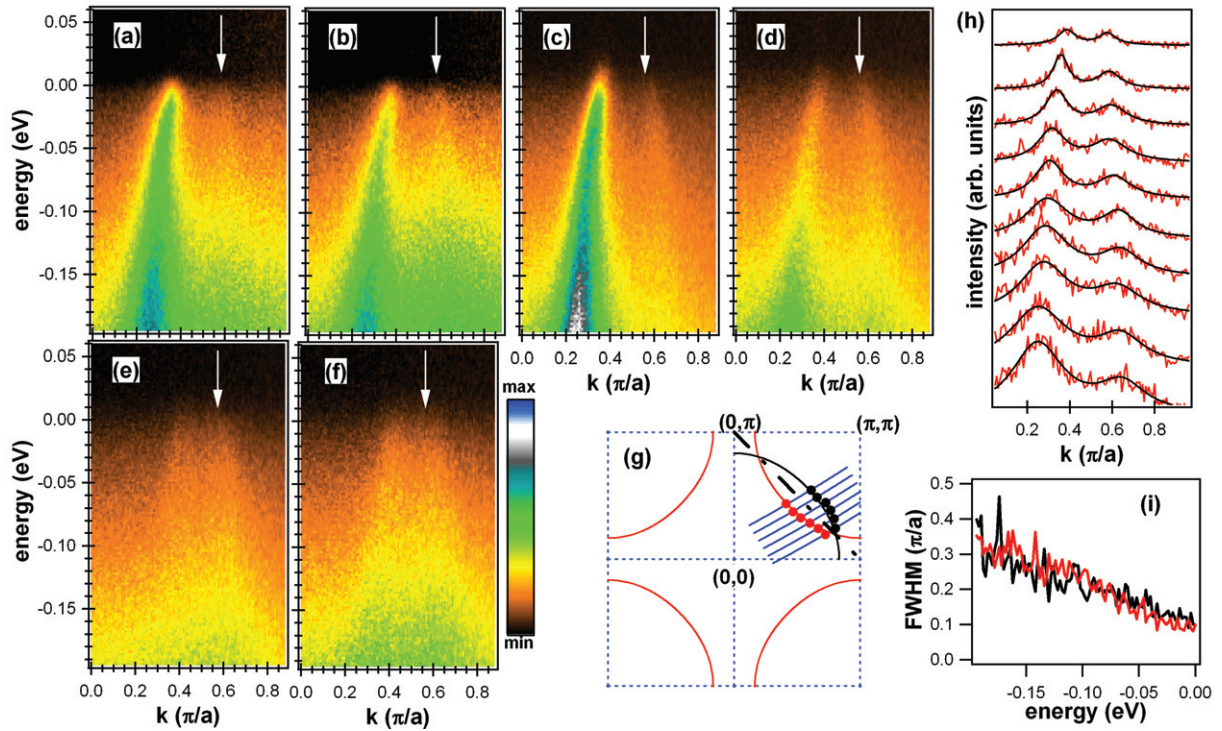
The presence of shadow bands in the cuprate superconductors is a well-known phenomenon for both Bi- and La-based compounds [17–19]. We have previously correlated the existence of a  $(\pi, \pi)$  folded shadow band in  $\text{La}_{2-x}\text{Sr}_x\text{CuO}$  and  $\text{La}_{2-x-y}\text{Nd}_y\text{Sr}_x\text{CuO}_4$  samples, close to the so-called 1/8-anomaly [20]. Such a folded band resembles the shadow band of Bi-based cuprates, but for LSCO a stronger doping dependence has been reported [21].

Here, we have observed the  $(\pi, \pi)$  folded band in the ARPES spectra of LSCO. The appearance of the folded band depends on the doping values of the samples. For the highly overdoped sample ( $x = 0.22$ ), we have only observed the main band, with the corresponding FS being electron-like. The  $(\pi, \pi)$  folded band first appears in the ARPES spectra of LSCO with  $x = 0.12$ . Figures 4(a)–(f) show the spectra taken from the  $\text{La}_{1.88}\text{Sr}_{0.12}\text{CuO}_4$  sample along



**Figure 4.** (a–f) ARPES intensity plots of LSCO ( $x = 0.12$ ) along the cuts (from left to right) shown in (g). The data were obtained at  $T = 12$  K. White arrows indicate the folded band. (g) Red curves are FS of the main band and the black curve is a copy of the main FS, but shifted by  $\mathbf{q} = (\pi, \pi)$ . The dashed line is the  $(\pi, \pi)$  BZ boundary. Blue lines indicate the momentum cuts. Red and black circles are  $k_f$  of the main and folded bands, respectively, as determined from MDCs at zero binding energy.

selected momentum cuts indicated in figure 4(g). Data were acquired in the second BZ but are presented in the first BZ, for convenience. The  $k_f$  of the folded band are symmetric to that of the main band about the  $(\pi, \pi)$  BZ boundary, i.e. they lie on a curve that copies the main FS but shifted by  $\mathbf{q} = (\pi, \pi)$ . Such a  $(\pi, \pi)$  folded band has also been observed in the superconducting sample with lower doping ( $x = 0.08$ ) (see figure 5). The  $k_f$  of the folded band can be traced to near the ‘hot spot’—the intersection between the FS of the main band and the  $(\pi, \pi)$  BZ boundary. From double Lorentzian fits we obtain similar MDC widths, as a function of energy, for the main and the folded bands (figures 5(h)–(i)). The FSs of the main and the folded bands form an enclosed loop that resembles a hole-like Fermi pocket in the nodal region. We have carried out measurements along cuts in different directions in the first, second and third BZs, but we did not find the  $(\pi, \pi)$  folded band in the region where the main band is occupied. The appearance of the  $(\pi, \pi)$  folded band depends on the doping. In the non-superconducting sample ( $x = 0.03$ ), the folded band was not observed in our measurements; either it does not exist or it is too weak to be observed.



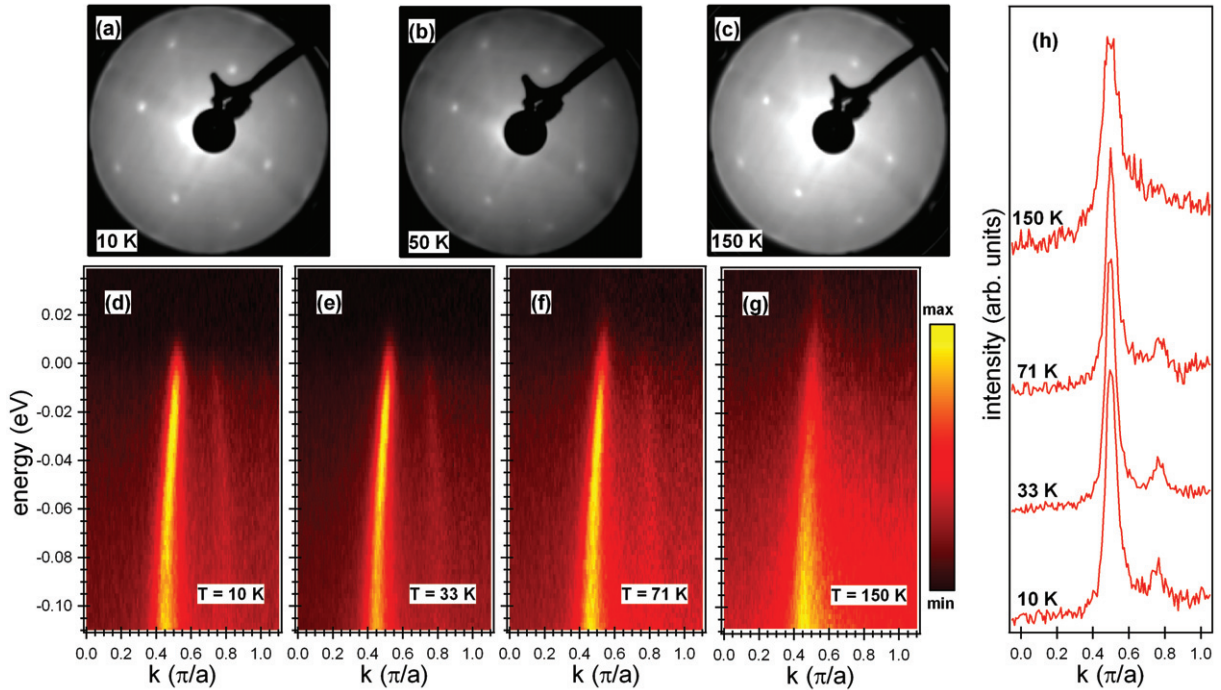
**Figure 5.** (a–f) ARPES intensity plots of LSCO ( $x = 0.08$ ) along the cuts (from top to bottom) shown in (g). The data were acquired at  $T = 12$  K. White arrows indicate the folded band. (g) Red curves are FS of the main band and the black curve is a copy of the main FS, but shifted by  $\mathbf{q} = (\pi, \pi)$ . The dashed line is the  $(\pi, \pi)$  BZ boundary. Blue lines indicate the momentum cuts. Red and black circles are  $k_f$  of the main and folded bands, respectively, as determined from MDCs at zero binding energy. (h) MDCs from  $-180$  meV (bottom) to  $0$  meV (top), taken from the intensity plot shown in (d), each curve is offset for clarity. The black lines are the fits with double Lorentzians. (i) The MDC peak widths of the main (red) and the folded (black) band, as a function of energy.

Figure 6 shows the main and  $(\pi, \pi)$  folded bands of the  $x = 0.08$  sample ( $T_c = 20$  K) at various temperatures. For temperatures up to 71 K, the folded band is clearly visible in the MDCs at the binding energy of 25 meV. At 150 K, the situation is less clear due to the thermal broadening of the MDC widths. The MDC peak from the folded band therefore becomes a shoulder on the intense peak. It is therefore hard to tell at what temperature the  $(\pi, \pi)$  folded band disappears. On the other hand, there is no experimental evidence for a structural modification from LEED on the same sample for temperatures up to 150 K.

#### 4. Discussion

While the FS of the main band changes systematically with doping values, the appearance of the  $(\pi, \pi)$  folded band shows unusual doping dependence. On increasing  $x$  to add more holes to the parent compound, the hole-like FS of the main band encloses an increasingly large area and eventually it becomes an electron-like FS, centered at the  $\Gamma$  point. The evolution of the FS with





**Figure 6.** (a–c) LEED patterns of LSCO ( $x = 0.08$ ) at 10, 50 and 150 K. (d–g) ARPES intensity plots of LSCO ( $x = 0.08$ ) at various temperatures along the cut indicated in figure 1(f). (h) The MDCs (each curve is offset for clarity) at  $-25$  meV, as a function of temperature.

doping is consistent with that observed in other cuprates [22, 23] by ARPES and with previous studies of LSCO [15]. In contrast to the monotonic change of the main band with doping, the folded band appears at a limited doping range.

It is difficult to explain the appearance of the  $(\pi, \pi)$  folded band (figures 4 and 5) at dopings below the 1/8-anomaly with the interpretation of the shadow band in Bi-based cuprates, which was proven as due to orthorhombic distortions of the crystal structure from tetragonality [24]. The arguments are: (a) LSCO has an orthorhombic lattice structure at low temperatures for  $x < 0.21$  [25], but the appearance of the  $(\pi, \pi)$  folded band has a clear onset at  $x \leq 1/8$ , and above this doping the  $(\pi, \pi)$  folded band was not observed; (b) at low temperatures the  $(\pi, \pi)$  folded band was also observed near the 1/8-anomaly in  $\text{La}_{1.48}\text{Nd}_{0.4}\text{Sr}_{0.12}\text{CuO}_4$  that has the low-temperature tetragonal structure, and it is insensitive to the transition from the low-temperature tetragonal structure to the low-temperature orthorhombic structure [20]. When the FS topology changes a so-called electronic topological transition (ETT) [26, 27] might occur, which would favor the formation of a charge or spin density wave instability [28] and could result in the appearance of the  $(\pi, \pi)$  folded band. However, the topology of the FSs changes at a doping between  $x = 0.17$  and  $x = 0.22$  that is far from the onset of the  $(\pi, \pi)$  folded band at  $x \leq 1/8$ . Near the 1/8-anomaly a wide variety of magnetic phenomena have been observed in La-based cuprates. However, it is not easy to reconcile those phenomena with the appearance of the  $(\pi, \pi)$  folded band because the corresponding orderings are different from  $\mathbf{q} = (\pi, \pi)$  [29]–[31]. For example, for the anti-phase striped state the  $\mathbf{q}$  vectors corresponding to the spin and charge patterns are  $(3\pi/4, \pi)$  and  $(\pi/2, 0)$ , respectively [13]. The appearance of the  $(\pi, \pi)$  folded band

suggests a unit cell doubling. In this regard, the  $(\pi, \pi)$  folded band would conform to the back folding of the main band about the new zone boundaries, the  $(\pm\pi, 0)$ – $(0, \pm\pi)$  lines. In terms of the location, the hole-like Fermi pocket enclosed by the main and  $(\pi, \pi)$  folded FSs would be consistent with that predicted from  $d$ -density wave (DDW) [32]. In the DDW ‘hidden order’ scenario, there is no net charge modulation, which would be compatible with the LEED patterns that do not show a supermodulation of charge with the appearance of the  $(\pi, \pi)$  folded band (figure 6). However, one obvious discrepancy is that DDW predicts a vanished spectral weight of the folded band near the zone diagonal, which is in disagreement with our measurements (figures 4 and 5).

Regardless of the exact origin of the  $(\pi, \pi)$  folded band, it is interesting to note that this folded band in our measurements appears in the superconducting samples that have doping values within the range at which multiple Fermi pockets are observed in  $\text{YBa}_2\text{Cu}_3\text{O}_{6+x}$  in quantum oscillation measurements. To account for the different observations of ARPES and quantum oscillation measurements in underdoped cuprates, various scenarios of an FS reconstruction have been proposed. Field-induced spin modulation [12], DDW [32] and striped state [13] have been invoked for the formation of the multiple Fermi pockets. The appearance of the  $(\pi, \pi)$  folded band and its similar MDC width compared to the main band (figures 6(h)–(i)) suggest that an FS reconstruction could already occur at zero magnetic field and at low temperatures, thus offering an additional possibility for explaining the multiple Fermi pockets. Indeed, a ‘hole-like’ pocket located near  $(\pi/2, \pi/2)$  with an enclosed area approximately corresponding to the hole concentration of the sample was inferred from the oscillation frequency of about 1600 Tesla in a recent quantum oscillation measurement [33] on  $\text{YBa}_2\text{Cu}_3\text{O}_{6+x}$ , which would be consistent with the hole-like pocket enclosed by the main band and its  $(\pi, \pi)$  folding. However, the small electron-like pocket(s) deduced from the lower frequencies in quantum oscillations was not identified in our present ARPES measurements. The  $(\pi, \pi)$  folded band was observed in the region of  $k$ -space where the main band is unoccupied, but not in the occupied part. In the case of the  $(\pi, \pi)$  band folding, an electron-like pocket is expected to occur at the anti-nodal region. Because the folded band is much weaker than the main band, it may be buried in the large spectral weight of the main band, especially in the anti-nodal region where the energy band is very shallow and flat (figure 2). It is therefore worth further exploring the details of the folded band by using different experimental settings (photon energy, polarization of light and the geometry of the measurement), aiming to maximize the intensity ratio between the folded band and the main band.

## 5. Summary

We have performed a systematic study of the electronic structure of LSCO by ARPES. In addition to the main band that changes monotonically with doping, we show that the band folding has unusual doping dependence. For superconducting samples with doping levels below the 1/8-anomaly, a  $(\pi, \pi)$  folded band was observed, which disappears at higher doping ( $x = 0.14$ ). This wavevector suggests a unit cell doubling. The appearance of the  $(\pi, \pi)$  folded band both at zero magnetic field and at low temperatures offers an additional possibility for the understanding of multiple Fermi pockets that were observed in quantum oscillation measurements in a similar doping range.

## Acknowledgments

This work was supported by the Swiss National Science Foundation (through NCCR, MaNEP and grant no. 200020-105151), the Ministry of Education and Science of Japan, the Swedish Research Council and the Foundation BLANCEFLOR Boncompagni-Ludovisi née Bildt. We thank the beamline staff of X09LA at the SLS for their excellent support.

## References

- [1] Campuzano J C, Norman M R and Randeria M 2004 Photoemission in the high  $T_c$  superconductors *Physics of Superconductors* vol 2, ed K H Bennemann and J B Ketterson (Berlin: Springer) p 167
- [2] Damascelli A, Hussain Z and Shen Z-X 2003 Angle-resolved photoemission of cuprate superconductors *Rev. Mod. Phys.* **75** 473–541
- [3] Plate M *et al* 2005 Fermi surface and quasiparticle excitations of overdoped  $\text{Tl}_2\text{Ba}_2\text{CuO}_{6+\delta}$  *Phys. Rev. Lett.* **95** 077001
- [4] Vignolle B *et al* 2008 Quantum oscillations in an overdoped high- $T_c$  superconductor *Nature* **455** 952
- [5] Doiron-Leyraud N *et al* 2007 Quantum oscillations and the Fermi surface in an underdoped high- $T_c$  superconductor *Nature* **447** 565
- [6] Sebastian S E *et al* 2008 A multi-component Fermi surface in the vortex state of an underdoped high- $T_c$  superconductor *Nature* **454** 200
- [7] Norman M R *et al* 1998 Destruction of the Fermi surface in underdoped high- $T_c$  superconductors *Nature* **392** 157
- [8] Kanigel A *et al* 2006 Evolution of the pseudogap from Fermi arcs to the nodal liquid *Nat. Phys.* **2** 447
- [9] Meng J *et al* 2009 Direct observation of Fermi pocket in high temperature cuprate superconductors *Nature* **462** 335
- [10] LeBouef D *et al* 2007 Electron pockets in the Fermi surface of hole-doped high- $T_c$  superconductors *Nature* **450** 533
- [11] Chen W-Q, Yang K-Y, Rice T M and Zhang F C 2008 Quantum oscillations in magnetic-field-induced antiferromagnetic phase of underdoped cuprates: application to ortho-II  $\text{YBa}_2\text{Cu}_3\text{O}_{6.5}$  *Europhys. Lett.* **82** 17004
- [12] Harrison N 2009 Spin-density wave Fermi surface reconstruction in underdoped  $\text{YBa}_2\text{Cu}_3\text{O}_{6+x}$  *Phys. Rev. Lett.* **102** 206405
- [13] Millis A J and Norman M R 2007 Antiphase stripe order as the origin of electron pockets observed in 1/8-hole-doped cuprates *Phys. Rev. B* **76** 220503
- [14] Mansson M *et al* 2007 On-board sample cleaver *Rev. Sci. Instrum.* **78** 076103
- [15] Yoshida T *et al* 2006 Systematic doping evolution of the underlying Fermi surface of  $\text{La}_{2-x}\text{Sr}_x\text{CuO}_4$  *Phys. Rev. B* **74** 224510
- [16] Yoshida T *et al* 2001 Electronlike Fermi surface and remnant  $(\pi, 0)$  feature in overdoped  $\text{La}_{1.78}\text{Sr}_{0.22}\text{CuO}_4$  *Phys. Rev.* **63** 220501
- [17] Aebi P *et al* 1994 Complete Fermi surface mapping of  $\text{Bi}_2\text{Sr}_2\text{CaCu}_2\text{O}_{8+x}$  (001): coexistence of short range antiferromagnetic correlations and metallicity in the same phase *Phys. Rev. Lett.* **72** 2757
- [18] Nakayama K *et al* 2006 Shadow bands in single-layered  $\text{Bi}_2\text{Sr}_2\text{CuO}_{6+\delta}$  studied by angle-resolved photoemission spectroscopy *Phys. Rev. B* **74** 054505
- [19] Zhou X J *et al* 2007 Angle-resolved photoemission spectroscopy on electronic structure and electron-phonon coupling in cuprate superconductors *Handbook of High-Temperature Superconductivity: Theory and Experiment* ed J R Schrieffer (Berlin: Springer) pp 87–144
- [20] Chang J *et al* 2008 Electronic structure near the 1/8-anomaly in La-based cuprates *New J. Phys.* **10** 103016
- [21] He R-H *et al* 2009 Doping dependence of the  $(\pi, \pi)$  shadow band in La-based cuprates studied by angle-resolved photoemission spectroscopy arXiv:0911.2245v1

- [22] Mesot J *et al* 2001 On the determination of the Fermi surface in high- $T_c$  superconductors by angle-resolved photoemission spectroscopy *Phys. Rev. B* **63** 224516
- [23] Kaminski A *et al* 2006 Change of Fermi-surface topology in  $\text{Bi}_2\text{Sr}_2\text{CaCu}_2\text{O}_{8+\delta}$  with doping *Phys. Rev. B* **73** 174511
- [24] Mans A *et al* 2006 Experimental proof of a structural origin for the shadow Fermi surface of  $\text{Bi}_2\text{Sr}_2\text{CaCu}_2\text{O}_{8+\delta}$  *Phys. Rev. Lett.* **96** 107007
- [25] Wakimoto S 2006 Incommensurate lattice distortion in the high temperature tetragonal phase of  $\text{La}_{2-x}(\text{Sr},\text{Ba})_x\text{CuO}_4$  *J. Phys. Soc. Japan* **75** 074714
- [26] Bruno E *et al* 1994 Fermi surfaces and electronic topological transitions in metallic solid solutions *Phys. Rep.* **249** 354
- [27] Varlamov A A *et al* 1989 Kinetic properties of metals near electronic topological transitions *Adv. Phys.* **38** 569
- [28] Gabovich A M *et al* 2001 Charge- and spin-density-wave superconductors *Supercond. Sci. Technol.* **14** R1
- [29] Tranquada J M *et al* 2004 Quantum magnetic excitations from stripes in copper oxide superconductors *Nature* **429** 534–8
- [30] Fujita M *et al* 2004 Stripe order, depinning, and fluctuations in  $\text{La}_{1.875}\text{Ba}_{0.125}\text{CuO}_4$  and  $\text{La}_{1.875}\text{Ba}_{0.075}\text{Sr}_{0.050}\text{CuO}_4$  *Phys. Rev. B* **70** 104517
- [31] Baledent V *et al* 2010 Two-dimensional orbital-like magnetic order in the high-temperature  $\text{La}_{2-x}\text{Sr}_x\text{CuO}_4$  superconductor *Phys. Rev. Lett.* **105** 027004
- [32] Chakravarty S and Kee H Y 2008 Fermi pockets and quantum oscillations of the Hall coefficient in high-temperature superconductors *Proc. Natl Acad. Sci. USA* **105** 8835
- [33] Sebastian S E *et al* 2010 Compensated electron and hole pockets in an underdoped high- $T_c$  superconductor *Phys. Rev. B* **81** 214524